Comparison of demand calibration in water distribution networks using pressure and flow sensors

Gerard Sanz

November 11, 2015

Abstract

Water distribution network models are used by water companies in a wide range of applications. A good calibration of these models is required in order to improve the confidence of the application results. Pressure and flow measurements are the main source of information when calibrating a hydraulic model. The selection of both the type and location of the sensors is crucial to guarantee a good calibration. This paper describes a sensor placement methodology based on the analysis of pressure and flow sensitivity using the Singular Value Decomposition. A comparison of demand calibration in a real network with synthetic data is presented. Three sets of sensors are considered: pressure sensors, flow sensors, and a combination of both.

1 Introduction

During the last decades, the concern about the water crisis has increased. Among many causes, inefficiencies in supply networks produce a loss of energy and water. These losses have an economic cost that water utilities can reduce. Network optimization [Creaco et al.(2015)] and fault detection and location [Pérez et al.(2014)] in water distribution networks (WDN) are two actions that can be performed to reduce the water and energy losses. Many of these techniques require a well calibrated model to generate reliable results [Savic et al.(2009)]. Model calibration consists in tuning the network parameters to reduce the error on predicted measurements. These measurements consist of pressure and/or flow sensors. Flow data are more sensitive to changes on demands and leakage appearance. However, their installation is much more expensive than pressure monitoring [Walski et al.(2014)]. Consequently, water utilities opt for installing pressure sensors, which have already been used for multiple purposes [Pérez and Sanz(2014)].

Many works in literature have treated the sampling design (i.e. sensor placement) problem. [Pinzinger et al.(2011)] proposed three algorithms based on integer linear programming and Greedy paradigm. [Kapelan et al.(2003)] solved a

multiobjective optimization using genetic algorithm (GA) for WDN model calibration. [Behzadian et al.(2009)] combined GA and adaptive neural network in a multi-objective optimization for WDN calibration. [Pérez et al.(2009)] used the GA to select sensors for leakage localization.

This work presents an assessment to determine: 1) what WDN model predicted variables (pressure and/or flow) to observe; and (2) where in the WDN to observe them. The parameters to be calibrated are the demand components values explained in [Sanz and Pérez(2015)], which represent geographical demand behaviours. The methodology to select the best sensors (pressure and/or flow sensors) is based on the analysis of the Singular Value Decomposition (SVD) of the WDN sensitivity matrix. The A, D, and V-optimalities of the sampling design solutions given by the methodology will be analysed to evaluate how well these solutions represent the true behaviour of the WDN. Finally, the validation of the calibrated demand components model for each set of selected sensors is performed by calculating the flow and pressure prediction error in 32 pipes and 34 nodes, respectively.

2 Problem Statement

Nodes in WDN models represent an aggregation of multiple demands. Each of these demands may be of different type, e.g. domestic, commercial, etc. Users of the same type are usually assumed to consume water in the same (i.e. similar) way, following a certain, usually pre-determined, diurnal demand pattern. The consumption of each user is then computed by multiplying the pattern coefficients with the baseline (i.e. average) demand. Once this is done, demands of different type that are associated with a certain network node are aggregated resulting in the total nodal consumption at a given point in time.

However, the information on different types of users associated with a given network node and their diurnal patterns and baseline demands is not always available in practice. Quite often, the only information available is the consumption aggregated during a period of time (usually monthly or quarterly). This low temporal resolution information on demands can still be used to compute the base demand of each consumer. The base demand of a node is computed from the sum of the base demands of consumers aggregated in this node. The basic model presented in Eq. 1 uses the nodal base demands, together with the total network consumption metered at the network inputs, to calculate the demand of each node at each sample.

$$\mathbf{d}_i(t) = \frac{bd_i}{\sum_{j=1}^{n_d} bd_j} \cdot \mathbf{q_{in}}(t) \tag{1}$$

where bd_i is the base demand of node i, n_d is the number of nodes in the network, and $\mathbf{q_{in}}(t)$ is the total network consumption metered at sample t.

The basic demand model (Eq. 1) cannot explain the daily variation of the relative pressure behaviour between two areas in the network. The demand

model in Eq. 2 presents a new approach to model demands depending on their geographical location.

$$\mathbf{d}_i(t) = \frac{bd_i}{\sum_{j=1}^{n_d} bd_j} \mathbf{c}_{j \to i}(t) \cdot \mathbf{q_{in}}(t) \tag{2}$$

where $\mathbf{c}_{j \to i}(t)$ is the value of the demand component j associated to node i depending on the node location. Demand components are calibrated demand multipliers that represent the behaviour of nodes in a determined geographical zone, avoiding the dependency on information of the user type and diurnal pattern behaviour. All nodes in the same area of node i have the same associated demand component. Consequently, all nodes in the same zone will have the same demand behaviour, weighted depending on their base demand. This demand model is capable of generating pressure variations in different zones of the network, as it happens in a real situation. However, the assumption that all nodes in the same area behave exactly in the same way is not realistic. For example, a node in the limit of the effect zone of two demand components should probably have a combination of the behaviour of the two demand components, instead of only one. To solve that, we can redefine the demand model in Eq. 2 so that the level to which each demand component is associated with each node is given as a membership, which depends on their geographical location. Eq. 3 represents the new demand model:

$$\mathbf{d}_i(t) = \frac{bd_i}{\sum_{j=1}^{n_d} bd_j} \cdot \mathbf{q_{in}}(t) \cdot (\alpha_{i,1} \cdot \mathbf{c}_1(t) + \alpha_{i,2} \cdot \mathbf{c}_2(t) + \cdots + \alpha_{i,n_c} \cdot \mathbf{c}_{n_c}(t)) \tag{3}$$

with

$$\sum_{j=1}^{n_c} \alpha_{i,j} = 1 \quad \forall i$$

where $\alpha_{i,j}$ is the association of demand component j with node i, and n_c is the number of demand components. The membership of each node to each demand component depends on the geographical location of the node, and is computed by means of the sensitivity analysis detailed in [Sanz and Pérez(2015)]. The model in Eq. 3 is capable of generating different behaviours in every demand, while only having to calibrate few (n_c) demand components.

[Sanz and Pérez(2015)] present the demand component calibration process using a least squares (LS) based procedure. At each sample, demand components values are estimated so that the errors in predicted measurements are minimized. This way of calibrating demands incorporates the usually ignored fact that demands depend in some ways of head status of the network. For example, if the pressure in a specific zone of the DMA decreases, the calibration process estimates demand component values that decrease the consumption of nodes in that zone. Demand components in this work should not be confused with the ones defined by [Giustolisi and Walski(2012)], where they were generated with a previous knowledge of the use of water (human-based, volume-based, non-controlled orifice-based, leakage-based).

The calibrated demand components generate individual demands that may not be exactly as the real ones, but the aggregated demand in a zone at a specific sample, and the cumulative demand of each individual node during a period of time (similar to the billing) will coincide with the real ones if other parameters (roughness, valve status, etc.) are well calibrated.

A comparison of the calibration results between type of user-based demand patterns and pressure sensitivity-based demand components is presented in [Sanz and Pérez(2014)], with better results for the latter: the uncertainty in the calibrated parameters is reduced, while the geographical distribution is useful for applications requiring parameters to be related with zones of the network. [Sanz and Pérez(2015)] also present the methodology to select the pressure sensors that have high sensitivity to one demand component while being low sensitive to the rest. This methodology will be used in this work to select both the pressure and flow sensors. This work considers the following assumptions:

- Pressures at the network inputs and total consumption are known.
- Noise is considered in the measurements.
- Quarterly billing for each individual consumer is known.
- The methodology is applied to a real network with synthetic data where uncertainty in demands is considered.
- Gross errors in field data and model are considered to be corrected at a prior stage.
- Status of valves in the DMA have been checked as part of the prior calibration process.

The calibration in this work is performed by means of a LS-based methodology, but other calibration methodologies can be used (e.g. GA). The sampling design procedure presented selects the sensors to calibrate demand components, but the same procedure can be applied if other parameters have to be calibrated.

3 Methodology

The methodology proposed analyses the information of the SVD of the sensitivity matrix $\mathbf{S}$ in order to select the sensors that give the highest information to calibrate the chosen parameters. The sensitivity matrix coefficients (i.e. the partial derivatives of head and flow with respect to each of the parameters) can be computed using the methods explained in [Yeh(1986)]: (1) Influence coefficient method; (2) Sensitivity equation method; and (3) Variational method. All three methodologies require $n+1$ simulations to be run in order to compute the complete sensitivity matrix, where n is the number of parameters in the model. [Cheng and He(2011)] propose a matrix analysis of the WDN linearized model where only one simulation is required at each iteration. The work presented uses the latter approach to compute the sensitivity matrix, but other techniques can be applied.

3.1 The Singular Value Decomposition

The SVD is capable of solving under-, over-, even- or mixed-determined problems with no rank conditions in $\mathbf{S}$, as explained by [Menke(1982)]. The SVD of matrix $\mathbf{S}$ with dimensions m x n is:

$$\mathbf{S} = \mathbf{U} \cdot \mathbf{\Lambda} \cdot \mathbf{V}^T \tag{4}$$

where $\mathbf{U}$ is a m x m matrix of orthonormal singular vectors associated with the m observed data, $\mathbf{V}$ is a n x n matrix of orthonormal singular vectors associated with the n system parameters; and $\mathbf{\Lambda}$ is a m x n diagonal matrix of singular values of $\mathbf{S}$, where the additional rows (more measurements than parameters) or columns (more parameters than measurements) are filled with zeros.

3.2 Sensor placement

As the objective of selecting sensors is to calibrate a WDN model, the number of sensors n_s is chosen to be equal to the number of parameters n_p in order to have an equally determined system of equations that guarantees the system identifiability.

Initially, matrix $\mathbf{U_r}$ is constructed with the first n_p columns of $\mathbf{U}$, as the information from the subsequent columns is negligible (they are multiplied by null rows of the $\mathbf{\Lambda}$ matrix). Then, the information density matrix $\mathbf{I_d}$ is computed as $\mathbf{I_d} = \mathbf{U_r}\mathbf{U_r}^T$ [Aster et al.(2005)], describing how the generalized inverse solution smears out the original data $\mathbf{y}$ into a predicted data $\hat{\mathbf{y}}$. Since $\mathbf{I_d}$ has been constructed from n_p orthonormal vectors in $\mathbf{U_r}$, a set of $n_p(=n_s)$ orthonormal vectors can be extracted from $\mathbf{I_d}$ in a way that they enhance the delta-like behavior of the $\mathbf{I_d}$ matrix [Wiggins(1972)]. This "*delta-like*" vector generation process is presented in Pseudo-code 1 (lines 1-6). The sensor with highest information is selected in line 3. The orthonormal vectors $\mathbf{u}^*$ are computed in line 4. In line 5, the chosen sensor and all the sensors with similar geometric directions (i.e. similar sensitivity coefficients) are deleted from the information density matrix, preparing it for the selection of the next sensor. This process results in a set of delta-like vectors $\mathbf{u}^*$ that form matrix $\mathbf{U}^*$. Subsequently, the rows of matrix $\mathbf{U}^*$ are normalised (line 7), so that sensors with high sensitivity to two parameters will not be selected. Finally, the sensor with highest value in each of the n_s columns is selected as the sensor with highest information density to calibrate a particular parameter (line 9).

Pseudo-code 1 uses the sensitivity matrix computed at a particular working point. In order to make the sensor placement process more robust, the procedure can be applied k times with k different working points. This results in a maximum of $k \cdot n_s$ possible sensor locations, from which n_s sensors have to be selected. Generally, the network topology has the highest impact on the sensitivity matrix, hence normally the sensors chosen at each working point are placed in near or same locations. The repetition r_i of a particular sensor is the number of times that this sensor location has been chosen, with a maximum of $r_i = k$. Fig. 1.a presents an example of all the possible sensors locations (and

Pseudo-code 1 Delta-like vector generation process for sensors selection

Require: $\mathbf{U_r}$, n_s
Compute $\mathbf{I_{d\,1}} = \mathbf{U_r}{\mathbf{U_r}}^T$
for $z = 1 : n_s$ **do**
  Find $j = max(diag(\mathbf{I_{d}}_z))$
  Compute $\mathbf{u}_z^* = \mathbf{i_{d}}_j / \sqrt{I_{d\ jj}}$
  Compute $\mathbf{I_{d}}_{z+1} = \mathbf{I_{d}}_z - \mathbf{u}_z^* \cdot \mathbf{u}_z^{*T}$
end for
Normalise rows of $\mathbf{U}^*$
for $z = 1 : n_s$ **do**
  Find $\mathbf{s}_z = max(\mathbf{U}^*(:, z))$
end for
return : $\mathbf{s}$

their repetitions) after applying Pseudo-code 1 with 24 different working points. The procedure to select the n_s final sensors consists of 6 steps:

1. Generate matrix $\mathbf{D_c}$ with the crossed pipe distances from each possible sensor to the others. This results in a symmetric matrix, with zeros in the diagonal.

2. Binarize the matrix, replacing distances by "1" if the distances are lower than a predefined distance threshold d_{th}, or "0" otherwise.

3. Select the sensor with highest number of "1", i.e. the sensor with highest number of sensors within d_{th}. This sensor is the relating sensor in its set. Fig. 1.b shows an example of a group of sensors to be reduced.

4. For each sensor in the set, the weight $\mathbf{w}_s$ of that sensor is calculated depending on the distance d to the other sensors and the repetitions r of the other sensors in the set, and the sensor itself:

$$\mathbf{w}_s = \sum_{i=1}^{n_{ss}} \frac{r_i}{10^{\frac{d_{is}}{d_{max(s)}}}} \tag{5}$$

   where n_{ss} is the number of sensors in the current set; d_{is} is the distance between sensor s and sensor i; and $d_{max(s)}$ is the maximum distance between sensor s and all other sensors in the current set. Eq. 5 prioritizes sensors with a high number of repetitions that are close to sensors that also have a high number of repetitions. Note that the exponent $d_{is}/d_{max(s)}$ is always in the interval $[0, 1]$, thus the denominators of the fractions are in the interval $[1, 10]$: the lower the distance d_{is}, the lower the value in the denominator.

5. The sensor in the set with highest weight is chosen as the reference sensor. All the other sensors are deleted from the possible sensors list and their number of repetitions is added to the reference sensor (Fig. 1.c).

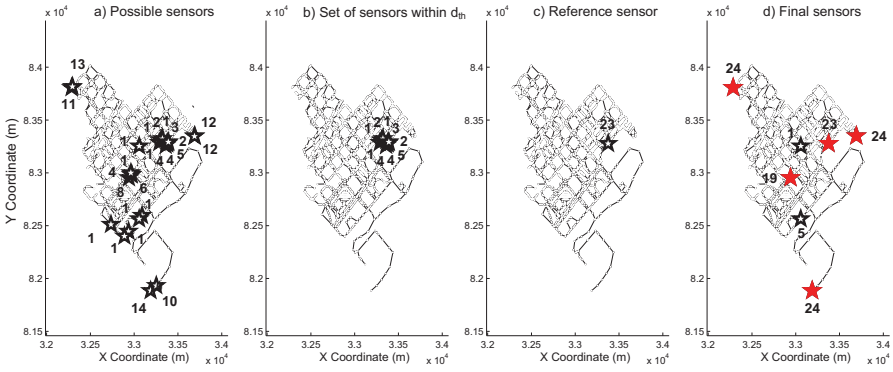

Figure 1: Example of the complete sampling design process: empty stars represent possible sensors; filled stars represent the selected sensors

6. Repeat step 1 until no sets of sensors appear in the binarised matrix.

This process generates a number of clusters depending on the defined threshold distance d_{th}. In the end, the n_s sensors with highest repetition number from the remaining set of sensors are chosen. Fig. 1.d shows all the possible sensors (stars), and the five selected sensors with highest repetitions (filled stars).

3.3 Optimality

The A, D and V-optimality criteria are used to evaluate how well a sampling design represents the true behaviour ('response') of a WDS. The A-optimality minimises the average parameter variance by minimising the trace of the inverse information matrix; the D-optimality maximises the determinant of the same matrix; and the V-optimality minimises the average prediction variance [Savic et al.(2009)]. In section 5, the optimality of the chosen sets of sensors using the methodology presented will be analysed by means of the formulas proposed by [Kapelan et al.(2003)], listed in Eq. 6.

$$F_1 = \frac{1}{n_p}\sum_{i=1}^{n_p}\mathbf{Cov}_{p,ii}^{1/2} \qquad F_2 = [det(\mathbf{S}^T\mathbf{W}\mathbf{S})]^{1/(2n_p)} \qquad F_3 = \frac{1}{n_z}\sum_{i=1}^{n_z}\mathbf{Cov}_{z,ii}^{1/2} \tag{6}$$

with

$$\mathbf{Cov}_p = \sigma^2 \cdot \mathbf{S}^T\mathbf{W}\mathbf{S} \qquad \mathbf{Cov}_z = \mathbf{S}_z \cdot \mathbf{Cov}_p \cdot \mathbf{S}_z^T \tag{7}$$

where $\mathbf{Cov}_p$ is the parameter covariance matrix; $\mathbf{W}$ is the weight matrix; n_z is the number of predicted variables of interest, i.e. the number of chosen predictions whose uncertainties are being evaluated; $\mathbf{Cov}_z$ is the prediction covariance matrix; σ^2 is the variance of the measures used to calibrate, considered the same for all measures; and $\mathbf{S}_z$ is the prediction sensitivity matrix, i.e. derivatives of

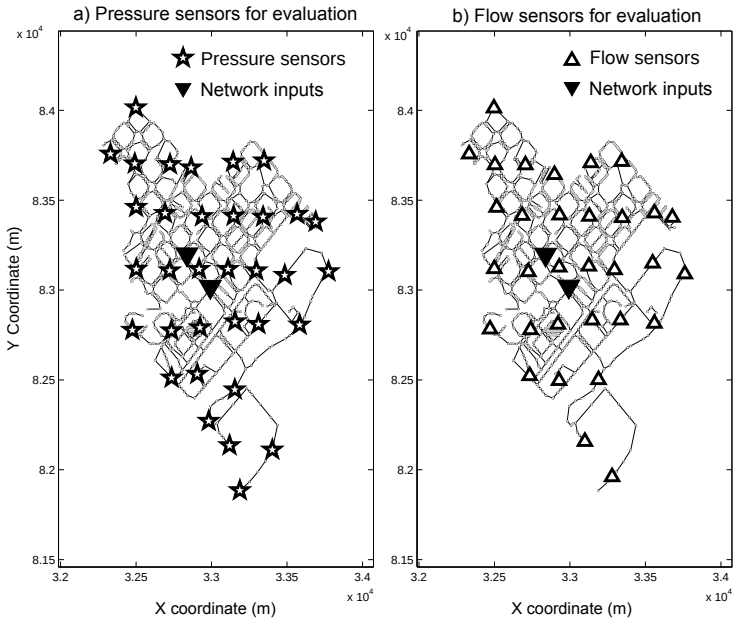

Figure 2: Nova Icaria DMA model with highlighted network inputs (inverted triangles) and sensors used to evaluate the calibrated model: a) Pressure sensors; and b) Flow sensors

head and flow predictions with respect to each of the parameters. F_1 and F_2 are based on the parameter uncertainty (A-optimality and D-optimality, respectively), while F_3 is based on the model prediction uncertainty (V-optimality).

4 Case Study

The methodology presented in the previous section is used to select different combinations of sensors in a real network model. These combinations will be used to calibrate the network using synthetic data. The network is a DMA situated in the Barcelona neighbourhood of Nova Icaria. It is composed of 3455 pipes and 3377 junctions, as depicted in Fig. 2. Water is supplied to the network through two pressure reduction valves, highlighted in Fig. 2 with inverted triangles. The total consumption of the DMA is supposed to be known, although the distribution of flows between both inlets is unknown. Pressure is monitored at both water inlets with a sample time of 10 minutes. The resolution for all pressure and flow sensors is 0.01 mwc and 0.01 l/s, respectively.

The calibrated model is validated using 34 pressure sensors and 32 flow sensors. The location of these sensors has been selected using a grid that covers all the DMA. The selected pressure and flow sensors are depicted with stars and

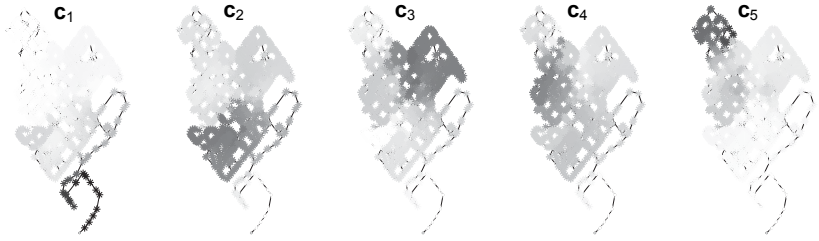

Figure 3: Representation of nodes' memberships to each demand component in scenario $Sc_{5,P}$

triangles in Fig. 2.a and Fig. 2.b, respectively.

4.1 Network parameterization

The distribution of parameters (demand components) is generated using the methodology presented in [Sanz and Pérez(2015)]. Three to six demand components are considered in order to analyse the results when having different number of sensors. Both the parameterization process (not included in this work) and the sampling design process depend on the type of sensors to be installed (pressure and/or flow), as the sensitivities involved are computed depending on the type of the sensors. This work presents the analysis of 12 different scenarios. Each scenario is denoted by $Sc_{n_s,T}$, where n_s is the number of sensors used and T is the type of sensors: F for flow, P for pressure and C for a combination of pressure and flow. Fig. 3 presents an example of the parameterization process output of scenario $Sc_{5,P}$, where five demand components have been defined from the pressure/demand sensitivity matrix. Each picture shows the memberships ($\alpha_{i,j}$ in Eq. 3) of nodes to a particular demand component: the darker the node, the higher the membership to that demand component.

5 Results

This section presents the results of the sensor placement methodology, the study of the optimality of the solution obtained in each scenario, and a summary of the calibration results.

5.1 Sensors placement

The methodology presented in section 3 has been applied to the case study network. Three to six sensors have been selected with 3 typologies: pressure sensors, flow sensors and combined sensors. Fig. 4 presents all the sensors in each scenario: a) 3 sensors; b) 4 sensors; c) 5 sensors; and d) 6 sensors. Pressure sensors distributed using the pressure/demand sensitivity matrix are depicted

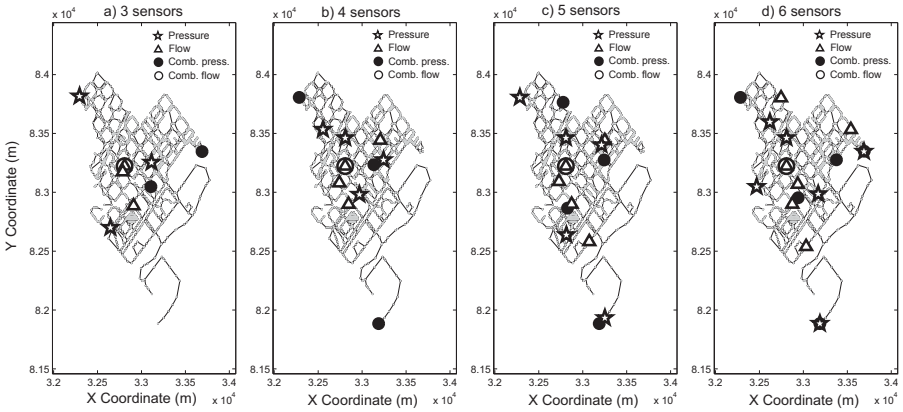

Figure 4: Sensor locations for pressure, flow and combined sensors: a) 3 sensors; b) 4 sensors; c) 5 sensors; and d) 6 sensors

as stars. Flow sensors distributed using the flow/demand sensitivity matrix are depicted as triangles. Finally, sensors selected using the combined pressure and flow/demand sensitivity matrix are depicted as full (pressure sensors) and empty (flow sensors) circles, respectively. Note that each pressure sensor (stars) in Fig. 4.c is located in the area affected by a different demand component (Fig. 3). This happens in all the scenarios. Relating to flow sensors, the first sensor chosen is always placed at the input pipe. The remaining flow sensors tend to be placed in high diameter pipes. The combined approach was proposed after analysing the flow and pressure sensor placement solutions: the sensitivity matrix is constructed containing all possible pressure sensors and the input pipe where a flow meter is always placed when only considering flow sensors. Results in Fig. 4 show that the flow sensor is automatically selected before any pressure sensor (this condition is not fixed), and that the remaining pressure sensors try to cover the rest of the network.

5.2 Optimality analysis

The A, D and V-optimalities of the solutions from the sensor placement methodology are compared against a representative part of all other possible solutions (30k-40k of other sensor combinations) using the formulas presented in Eq. 6. The three types of optimalities are compared at 24 different samples (corresponding to 24 hours in a day). Tab. 1 sums up the percentage of sensors combinations with better optimalities than the one from the solution obtained by the methodology. The worst case out of the 24 hours analysed is presented for each optimality criterion.

Tab. 1 shows that flow sensors chosen by means of the methodology presented are the ones with highest percentage of other preferable sensors combinations, with a maximum of a 10.8% in the V-optimality criterion when selecting 6 flow

Table 1: Percentage of sensors combinations with better optimality (%) than the SVD solution

Scenario	A-Optimality	D-Optimality	V-Optimality
Sc_{3F}	1,224%	3,115%	3,104%
Sc_{3P}	0,600%	0,350%	0,813%
Sc_{3C}	0,003%	0,003%	0,350%
Sc_{4F}	0,259%	4,120%	8,358%
Sc_{4P}	1,656%	1,217%	2,206%
Sc_{4C}	0,003%	0,003%	0,003%
Sc_{5F}	0,056%	0,581%	0,950%
Sc_{5P}	0,036%	0,042%	0,053%
Sc_{5C}	0,003%	0,003%	0,006%
Sc_{6F}	0,003%	10,320%	10,859%
Sc_{6P}	0,015%	0,013%	0,015%
Sc_{6C}	0,003%	0,003%	0,021%

Table 2: Prediction Mean Squared Error for each scenario

		Basic model	Demand components model		
		No Calibration	Flow sensors	Pressure sensors	Combined sensors
3 sensors	MSE_{flow} (l^2/s^2)	0,000460	0,000675	0,000365	0,000376
	$\text{MSE}_{pressure}$ (m^2)	0,042237	0,059845	0,031743	0,032858
4 sensors	MSE_{flow} (l^2/s^2)	0,000460	0,000843	0,000417	0,000297
	$\text{MSE}_{pressure}$ (m^2)	0,042237	0,078316	0,043707	0,023512
5 sensors	MSE_{flow} (l^2/s^2)	0,000460	0,000243	0,000136	0,000265
	$\text{MSE}_{pressure}$ (m^2)	0,042237	0,013553	0,004128	0,018187
6 sensors	MSE_{flow} (l^2/s^2)	0,000460	0,000191	0,000136	0,000187
	$\text{MSE}_{pressure}$ (m^2)	0,042237	0,012351	0,004647	0,010427

sensors. The maximum value for pressure sensors is 2.2% of other preferable sensors combinations, also in the V-optimality criterion, for four pressure sensors. Finally, the maximum value for combined sensors is 0.35% of preferable sensors in the V-optimality criterion for three combined sensors.

5.3 Calibration performance

Tab. 2 presents the mean squared errors (MSE) between the real values measured at the locations described in section 4, and the predicted values using the basic demand model and the demand components model calibrated with 3-6 sensors with different typologies. A graphical representation of the data in Tab. 2 is found in Fig. 5.

Fig. 5 and Tab. 2 show that all the demand components models that have been calibrated using pressure or combined sensors improve the overall performance comparing to the basic model. When calibrating demand components by means of flow sensors, more than four sensors are required. The best result observed has been obtained when calibrating demand components using five pressure sensors, as introducing a sixth sensor does not improve the modelling error. In particular, the chosen sensors in scenario Sc_{5P} only has 0.036%-0.053% of

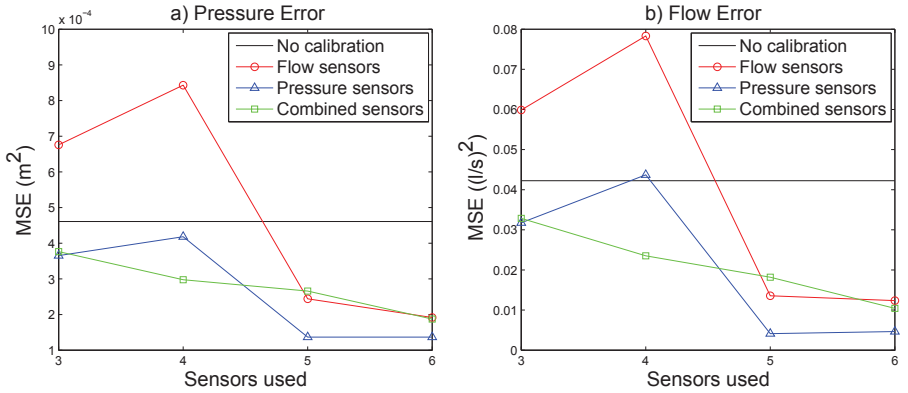

Figure 5: Calibration results for all scenarios: a) Pressure error; and b) Flow error

better sensors locations (regarding to all optimalities criteria), as seen in Tab. 1.

6 Conclusions

This work presents a sensor placement methodology that utilises the SVD of the WDN sensitivity matrix to select a set of sensors to calibrate pre-defined demand components. The method can be applied in multiple time samples to make the sensor placement process more robust, selecting the best sensors for a range of different working points. This can lead to different sensors locations at each time sample used. To solve that, a simple clustering procedure is proposed to decide which of the possible sensors are the most representative for all the range of working points.

The methodology is then applied to select twelve sets of sensors that comprise from three to six sensors, and combine pressure and/or flow sensors. Each of the twelve sets is used to calibrate a number of demand components equal to the number of sensors. Calibration results are evaluated by means of 32 flow sensors and 34 pressure sensors that have been distributed using a grill that covers all the DMA. It has been seen that as the number of demand components (and sensors) increase, the results obtained in terms of pressure and flow MSE at the evaluation sensors improve. Furthermore, results show that measuring pressure seems to be the best option when calibrating demand components, whereas metering flow requires a higher number of sensors to achieve a good calibration. This can be justified by the meshed topology of the network: pressure is more representative of a geographical zone, thus improving predicted pressure in a particular point of the network will improve predicted pressure in the nearby locations; on the other hand, improving the predicted flow at a particular pipe does not necessarily improves the rest of flows of the zone, due to the meshed

topology of the network.

Finally, the A, D and V-optimalities of the sets of sensors chosen have been computed and compared with the ones obtained from a representative number of all other possible combinations of sensors. The analysis shows that the optimalities obtained with the proposed methodology can be little improved when considering pressure sensors or a combination of flow and pressure sensors. The selection of flow sensors leads to good A-optimality, but slightly worse D and V-optimalities.

The results from the calibration evaluation and optimality analysis show that the proposed methodology can be a good and faster alternative to the application of GAs or exhaustive algorithms.

Future work will analytically justify the good results of the methodology in terms of the different optimalities. Besides, the combined distribution of flow and pressure sensors will not be restricted to only one flow sensor.

Acknowledgements

This work was supported in part by the project FP7 - ICT - 2012 - 318556 (EFFINET) of the European Commission, by the Project DPI2014 - 58104 - R (HARCRICS) of the Spanish Ministry of Education, by the Project DPI2013-48243-C2-1-R (ECOCIS) of the Spanish Ministry of Economy and Competitiveness, and by the Polytechnic University of Catalonia. The model of the real network was provided by the Barcelona Water Company AGBAR.

References

[Creaco et al.(2015)] E. Creaco, D. Ph, G. Pezzinga, Multiobjective Optimization of Pipe Replacements and Control Valve Installations for Leakage Attenuation in Water Distribution Networks, Journal of Water Resources Planning and Management (2015) 1–10.

[Pérez et al.(2014)] R. Pérez, G. Sanz, V. Puig, J. Quevedo, M. A. Cuguero Escofet, F. Nejjari, J. Meseguer, G. Cembrano, J. M. Mirats Tur, R. Sarrate, Leak Localization in Water Networks: A Model-Based Methodology Using Pressure Sensors Applied to a Real Network in Barcelona, IEEE Control Systems 34 (2014) 24–36.

[Savic et al.(2009)] D. Savic, Z. Kapelan, P. Jonkergouw, Quo vadis water distribution model calibration?, Urban Water Journal 6 (2009) 3–22.

[Walski et al.(2014)] T. Walski, P. Sage, Z. Wu, What Does it Take to Make Automated Calibration Find Closed Valves and Leaks?, World Environmental and Water Resources Congress 2014 (2014) 555–565.

[Pérez and Sanz(2014)] R. Pérez, G. Sanz, Optimal placement of metering devices for multiple purposes, in: 11th Int. Conference on HydroInformatics, NY, 2014.

[Pinzinger et al.(2011)] R. Pinzinger, J. Deuerlein, A. Wolters, A. Simpson, Alternative approaches for solving the sensor placement problem in large networks, in: Water Distribution Systems Analysis, 2011.

[Kapelan et al.(2003)] Z. Kapelan, D. Savic, G. Walters, Multiobjective Sampling Design for Water Distribution Model Calibration, Journal of Water Resources Planning and Management 129 (2003) 466–479.

[Behzadian et al.(2009)] K. Behzadian, Z. Kapelan, D. Savic, A. Ardeshir, Stochastic sampling design using a multi-objective genetic algorithm and adaptive neural networks, Environmental Modelling & Software 24 (2009) 530–541.

[Pérez et al.(2009)] R. Pérez, V. Puig, J. Pascual, A. Peralta, E. Landeros, L. Jordanas, Pressure sensor distribution for leak detection in Barcelona water distribution network, Water Science & Technology: Water Supply 9 (2009) 715.

[Sanz and Pérez(2015)] G. Sanz, R. Pérez, Sensitivity Analysis for Sampling Design and Demand Calibration in Water Distribution Networks Using the Singular Value Decomposition, Journal of Water Resources Planning and Management (2015).

[Giustolisi and Walski(2012)] O. Giustolisi, T. Walski, Demand Components in Water Distribution Network Analysis, Journal of Water Resources Planning and Management 138 (2012) 356–367.

[Sanz and Pérez(2014)] G. Sanz, R. Pérez, Comparison of Demand Pattern Calibration in Water Distribution Network with Geographic and Non-Geographic Parameterization, in: 11th International Conference on HydroInformatics, New York, 2014.

[Yeh(1986)] W. Yeh, Review of Parameter Identification Procedures in Groundwater Hydrology: The Inverse Problem, Water Resources Research (1986).

[Cheng and He(2011)] W. Cheng, Z. He, Calibration of Nodal Demand in Water Distribution Systems, JWRPM 137 (2011) 31–40.

[Menke(1982)] W. Menke, Geophysical Data Analysis: Discrete Inverse Theory, Academic Press, 1982.

[Aster et al.(2005)] R. Aster, B. Borchers, C. Thurber, Parameter Estimation and Inverse Problems, Elsevier, New York, 2005.

[Wiggins(1972)] R. Wiggins, The general linear inverse problem: Implication of surface waves and free oscillations for Earth structure, Reviews of Geophysics 10 (1972) 251–285.